ResearchGate

See discussions, stats, and author profiles for this publication at: https://www.researchgate.net/publication/6789375

Fabrication of Nanorattles with Passive Shell

ARTICLE *in* THE JOURNAL OF PHYSICAL CHEMISTRY B · NOVEMBER 2006

Impact Factor: 3.3 · DOI: 10.1021/jp061886h · Source: PubMed

CITATIONS
31

READS
17

6 AUTHORS, INCLUDING:

Hao Ming Chen
National Taiwan University
60 PUBLICATIONS **1,642** CITATIONS

SEE PROFILE

Kiyotaka Asakura
Hokkaido University
391 PUBLICATIONS **7,089** CITATIONS

SEE PROFILE

Ling-Yun Jang
National Synchrotron Radiation Research Ce…
140 PUBLICATIONS **1,603** CITATIONS

SEE PROFILE

Available from: Hao Ming Chen
Retrieved on: 23 January 2016

Fabrication of Nanorattles with Passive Shell

Hao Ming Chen,[†] Ru-Shi Liu,[*,†] Kiyotaka Asakura,[‡] Jyh-Fu Lee,[§] Ling-Yun Jang,[§] and Shu-Fen Hu[||]

Department of Chemistry, National Taiwan University, Taipei 106, Taiwan, Catalysis Research Center, Hokkaido University, Sapporo, Japan, National Synchrotron Radiation Research Center, Hsinchu 300, Taiwan, and Institute of Electro-optical Science and Technology, National Taiwan Normal University, Taipei 116, Taiwan

Received: March 27, 2006; In Final Form: August 8, 2006

This investigation describes the formation of a metal nanorattle with a pure metal shell by varying experimental parameters. The galvanic replacement reaction between silver and chloroauric acid was adopted to prepare hollow metal nanoparticles. This approach is extended to produce nanorattles of Au cores and Au shells by starting with $Au_{core}Ag_{shell}$ nanoparticles as templates. The effect of temperature on the nanostructure of the final product is also considered. The composition of the shell in nanorattles can be controlled by varying the reaction temperature (to form pure gold or gold−silver alloy, for example). X-ray absorption fine structure spectroscopy is conducted to elucidate the fine structure of these nanoparticles. Partial alloying between the Au core and the Ag shell is observed by extended X-ray absorption fine structure (EXAFS).

Downloaded by NATIONAL TAIWAN UNIV on August 10, 2009
Published on September 13, 2006 on http://pubs.acs.org | doi: 10.1021/jp061886h

Introduction

The preparation and characteristics of bimetallic nanoparticles have received considerable attention, since the catalytic properties and electronic structures of such nanomaterials may be able to be tailored by altering their compositions and structures.[1] Silver or gold nanostructures have attracted substantial interest because of their widespread use in applications such as catalysis, photonics, electronics, optoelectronics, and biological sensing.[2] Specifically, the optical properties of Au/Ag bimetallic nanoparticles synthesized from free-electron-like metals have been extensively examined,[3−14] because of the collective oscillation of the free conduction electrons induced by an interacting electromagnetic field. These resonances are also called surface plasmon (SP). Surface plasmon extinction spectra of both Au−Ag core−shell[4−12] and alloy[13,14] particles were obtained for various nanoparticulate compositions. Au−Ag core−shell nanoparticles (with a Au or Ag core and a Ag or Au shell) are characterized by two extinction peaks at approximately 400 and 530 nm, while solid nanoparticles made of pure Ag or Au have only a single SP peak. Au−Ag alloy nanoparticles (Au and Ag atoms randomly distributed in single particles) exhibit only one surface plasmon band. The plasmon maximum, λ_{max}, is a linear function of Au−Ag composition. Hollow nanostructures are a particularly interesting class of materials that have unusual chemical and physical characteristics that are determined by their shape and composition. They have great potential in the development of novel and potentially useful sensing and drug-delivery applications.[15] Hollow nanospheres, cubes, rods, tubes, and triangular prisms have been successfully synthesized.[16−25] Transforming metal nanostructures into hollow structures improves their performance because their densities are lower and their surface areas higher than those of their solid counterparts. The hollow Pd spheres exhibited good catalytic activities in Suzuki cross-coupling reactions and can be reused numerous times without loss of catalytic activity.[26] The galvanic replacement reaction has been exploited as a powerful means of preparing hollow metal nanostructures. These metal nanostructures exhibit a number of interesting optical features.

The structural determination of metal nanostructures is important for future applications. The study of the extended X-ray absorption fine structure (EXAFS) has been particularly useful in providing structural information about the noncrystalline and the crystalline materials. EXAFS is a powerful tool for elucidating the local structure of the metal nanoparticles in colloidal dispersions and small metal particles. The measurements yield information on the environment of a particular atom in a metal cluster. For instance, the number and species of neighboring atoms and their distances from the X-ray absorbing atom can be determined without long range order. Toshima and co-workers reported both experimental and simulated coordination numbers of Au/Pd[27,28] and Pt/Pd[29] bimetallic clusters. This study reports a strategy for synthesizing a hollow nanostructure that is best described as a hollow nanorattle. First, a Au_{core}-Ag_{shell} structure was produced by the reduction of metal salts by trisodium citrate in the absence of polymer. A galvanic replacement reaction between silver shells and aqueous $HAuCl_4$ solution yielded nanorattles with Au cores and Au shells. Most interestingly, such a nanostructure differs from those previously reported.[24,25] A nanorattle comprises a Au shell rather than a Au/Ag alloy shell. Hence, this nanostructure exhibits a great passive ability. These new core/shell nanostructures with a noble metal shell are expected to find uses in various applications that may include plasmonics, sensing, and catalysis.

Experimental Section

Chemicals and Materials. Hydrogen tetrachloraurate(III) hydrate, trisodium citrate dehydrate (99%), silver nitrate (99%), and poly(vinyl pyrrolidone) (PVP, $M_w = 58\,000$) were obtained from Acros Organics and used without further purification. The water used throughout this investigation was reagent-grade

* Author to whom correspondence should be addressed. E-mail: rsliu@ntu.edu.tw.
[†] National Taiwan University.
[‡] Hokkaido University.
[§] National Synchrotron Radiation Research Center.
[||] National Taiwan Normal University.

10.1021/jp061886h CCC: $33.50 © 2006 American Chemical Society
Published on Web 09/13/2006

Downloaded by NATIONAL TAIWAN UNIV on August 10, 2009
Published on September 13, 2006 on http://pubs.acs.org | doi: 10.1021/jp061886h

water, produced using a Milli-Q SP ultrapure-water purification system from Nihon Millipore Ltd., Tokyo.

Preparation. Water was used as the solvent in all reactions, in which sodium citrate served as both the capping reagent and the reducing agent. For a typical preparation, the colloidal nanoparticles were prepared by adding 5 mL of sodium citrate (1%) to 50 mL of gold metal salt ($HAuCl_4$, 0.2 mM) solution. The solution was heated at 95 °C in an oil bath for 20 min, and then, 0.6 mL of 0.25 M $AgNO_3$ solution was added dropwise. The mixture was then allowed to react for another 30 min in an oil bath. The reaction mixture was centrifuged at 8000 rpm for 30 min to remove the excess reducing agent (sodium citrate). The solution was then allowed to cool before the replacement reaction was performed. The final product (Au colloids whose surfaces were coated with shells of pure Ag) were redispersed in 50 mL of water.

In the replacement experiment, an aliquot of 0.25 M $HAuCl_4$ (0.4 mL) solution was added dropwise to the new dispersion at room temperature. The mixture continued to undergo the reaction for another 20 min to yield nanoparticles with Au cores and Au shells. In the stability test of newly synthesized nanorattles, 1 mL of (0.25 M) $HAuCl_4$ solution and 5 mL of (1 M) HNO_3 were added to 50 mL of nanorattle solution. The solution of $HAuCl_4$ and $AgNO_3$ was prepared by dissolving the corresponding salts in water. Vigorous magnetic stirring was maintained throughout the synthesis.

Characterization of Nanoparticles. The UV−vis spectra of the colloidal nanoparticle solutions were obtained using a Shimadzu UV-1700 spectrophotometer with a 10 mm quartz cell at room temperature. The surface morphology of the samples was studied by transmission electron microscopy (TEM) (JEM-2010, 200 kV). The specimens were obtained by placing many drops of the colloidal solution onto a Formvar-covered copper grid and evaporating it in air at room temperature. Prior to specimen preparation, the colloidal solutions were sonicated for 1 min to improve the dispersion of particles on the copper grid. Elemental analysis was conducted using an inductively coupled plasma atomic emission spectrometer (Shimadzu ICPS-1000III) and an elemental analyzer (Flash EA 1112 series/CE Instruments).

The samples (used in the EXAFS measurement were prepared by concentrating 2000 mL of the previously obtained colloidal dispersions to 5−10 mL under nitrogen at reduced pressure. A series of EXAFS measurements of the synthesized samples were made using synchrotron radiation at room temperature. A few samples were required for such measurement. Colloidal nanoparticles dispersed well in solution. Measurements were made at the Au L_{III} edge (11 918 eV) and the Ag K edge (25 514 eV) with the sample held at room temperature.

EXAFS Data Analysis. Raw X-ray absorption data were analyzed following standard procedures,[30] including pre-edge and post-edge background subtraction, normalization with respect to edge height, Fourier transformation, and nonlinear least-squares curve fitting. The normalized k^3-weighted EXAFS spectra, $k^3x(k)$, were Fourier-transformed in the k range from 2.5 to 14 $Å^{-1}$ to reveal the contribution of each bond pair on the Fourier transform (FT) peak. The experimental Fourier-filtered spectra were obtained by performing an inverse Fourier transformation with a Hanning window function with r between 1.9 and 3.2 Å. The S_0^2 (amplitude reduction factor) values of the Au and Ag atoms were fixed at 0.8 and 0.83, to determine the structural parameters of each bond pair. Au and Ag edge data were analyzed simultaneously. The Debye−Waller factors, interatomic distance, and coordination numbers of Au−Ag and Ag−Au bonds were constrained to be equal in both analyses of Au L_3 and Ag K edges. Eight fitting parameters were used. They were two sets of the following four: the coordination number (N), interatomic distance (R), energy shift (ΔE), and Debye−Waller factor (DW) was less than N*par*, given by the equation $Npar = 2\Delta k\Delta r/\pi$, where Δk and Δr are the widths in k- and r-space used in the data analysis. The backscattering amplitude and phase shift functions for specific atom pairs were calculated ab initio using the FEFF7 code. The Wiggler-C beamline of the National Synchrotron Radiation Research Center (NSRRC), Taiwan, has been designed for such experiments.

SCHEME 1: Synthetic Routes of Nanorattles with Au Cores and Au Shells, Involving Galvanic Replacement

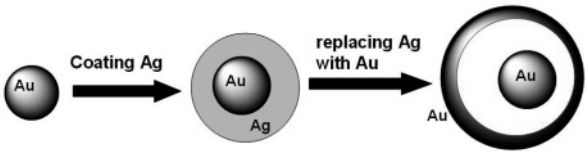

Synthesis and TEM Analysis of Each Product. A galvanic process was used to make nanorattles that consisted of Au cores and Au shells, by reacting $Au_{core}Ag_{shell}$ nanoparticles with $HAuCl_4$, in a water solution (Scheme 1). The first step involved the deposition of a uniform layer of pure silver on the surface of Au nanoparticles. $Au_{core}Ag_{shell}$ nanoparticles have been prepared by directly depositing Ag atoms on the surface of Au nanoparticles using ascorbic acid as a reducing agent.[24] In the present study, Au nanoparticles were mixed directly with an aqueous solution of sodium citrate and $AgNO_3$ at high temperature (95 °C). The high temperature is critical to the reduction of silver ions to atoms. The redox reaction between sodium citrate and silver ions cannot occur at room temperature. Silver ions were reduced by sodium citrate, yielding silver atoms, which nucleated and grew on the surfaces of gold nanoparticles. The similarities between both the atomic radii (Au = 1.44 Å; Ag = 1.45 Å) and lattice parameters (Au lattice constant a = 4.069 Å JCPDS file no. 01-1172; Ag lattice constant a = 4.079 Å JCPDS file no. 01-1164) of silver and gold cause the silver atoms to preferentially nucleate and grow on the surfaces of gold nanoparticles, rather than homogeneously nucleating and growing from silver nuclei. The success of seed-mediated growth methods is related to the promotion of autocatalytic growth over additional nucleation. The gold nanoparticles act as nucleation centers on whose surfaces grow Ag atoms, suggesting that the product was $Au_{core}Ag_{shell}$ (rather than single-component gold and silver nanoparticles). Notably, $Au_{core}Ag_{shell}$ nanoparticles cannot be fabricated using a strong and fast reducing agent (such as sodium borohydride) although more nuclei and nucleation can be formed. In the presence of a strong redcuing agent, the presence of seeds appears to promote the formation of seeds over growth. The nucleations are markedly enhanced over particle growth. In the presence of a weak reducing agent, the seeds grow.[31] Slowing the reduction of silver ions and the formation of silver atoms enables gold nanoparticles to be coated with silver shells.

The second step involved the galvanic replacement reaction between $Au_{core}Ag_{shell}$ colloids with an aqueous $HAuCl_4$ solution at room temperature, whose chemical reaction can be written as $3Ag + AuCl_4^- \rightarrow 3Ag^+ + 4Cl^- + Au$. A conformal coating of pure silver was transformed into a shell made of gold by galvanic replacement. The constituents of the shells of the newly synthesized nanorattles differed from those of hollow nanoparticles, reported elsewhere.[24,25] After conformal silver shells were replaced with $HAuCl_4$ solution, the hollow shells were made

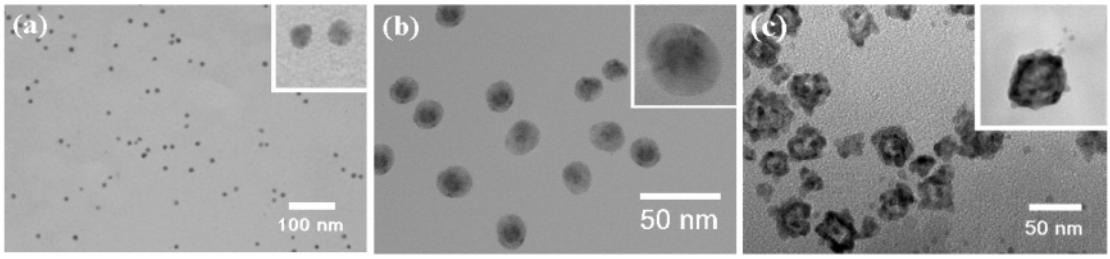

Figure 1. (a) TEM image of Au noparticles. (b) TEM image of Au colloids whose surfaces have been coated with shells of pure silver. (c) TEM image of nanorattles that had been prepared by adding $HAuCl_4$ solution to the colloids from part b.

of gold. However, the hollow shells, according to previous results, were transformed into a shell made of Au/Ag alloy via a galvanic reaction.[24,25] The difference between the results in this study and earlier results will be discussed below.

The nanostructures that are involved in each reaction step have been fully characterized using TEM. As displayed in Figure 1a, gold nanoparticles as small as 8.1 nm, with a standard deviation of 1.2 nm, were obtained. Figure 1b presents a typical TEM image of the $Au_{core}Ag_{shell}$ nanoparticles. The brightness in the image reflects the intensity of scattered electrons from various substances and is proportional to the atomic number (Z). In Figure 1b, the Au particles, which have a higher Z value than the Ag shell, are imaged as darker parts. The mean diameter was increased from ~8 to ~20 nm after silver coating. When the silver-coated nanoparticles underwent the galvanic replacement reaction with a solution of gold ions, the pure silver layers were transformed into gold nanoshells. Figure 1c shows a typical TEM image of the nanorattle. The image clearly revealed that the product was characterized by a rattlelike nanostructure. Notably, the core of the nanorattle shrunk slightly because the silver shell of $Au_{core}Ag_{shell}$ nanoparticles was not a perfect layer Au/Ag alloy (silver-rich), as verified by EXAFS analysis. Notably, some entities exhibited a weaker contrast than the Au shell attached to the surface of the gold shell. They were AgCl solids formed by galvanic replacement, as confirmed by elemental analysis (Supporting Information Table S1), which will be discussed later. The shell material and chemical reactivity of the newly synthesized nanorattles will play an important role in future applications and are investigated herein. Gold nanoparticles modified with oligonucleotides, for example, were adopted to indicate the presence of a particular DNA sequence hybridized on a transparent substrate.[2e]

EXAFS Analysis of Each Product. EXAFS was conducted to obtain better evidence of the structural parameters of Au/Ag bimetallic nanoparticles. Figure 2 displays the Au L_3 edge EXAFS oscillations of Au nanoparticles, Au colloids whose surfaces have been coated with shells of pure silver, and Au_{core}-Ag_{shell} nanoparticles whose Ag shells were replaced with $HAuCl_4$ solution. They correspond to parts a, b, and c of Figure 1, respectively. Notably, the change in oscillatory feature above approximately $k = 5.5$ Å^{-1} occurs when they are coated with the silver shell because of the presence of Ag near neighbors around Au atoms, in that Au and Ag have substantially varying phase shifts and amplitudes in the backscattering function with k. As indicated by the arrow, for Au colloids whose surfaces were coated with shells of pure silver (b), the spectral oscillation changed markedly with the coating with the silver shell. This large difference facilitates the coordination analysis of the Au−Ag system. Figure 3 presents the magnitude of the Fourier transform of $k^3\chi(k)$ for each sample, where $k = 2.5-14$ Å^{-1} is transformed. Evidently, a phase shift in $\chi(k)$ is seen, and Au−Ag in the first shell appears as a doublet in the Fourier transform of $\chi(k)$ (indicated by an arrow in Figure 3). The peak intensity

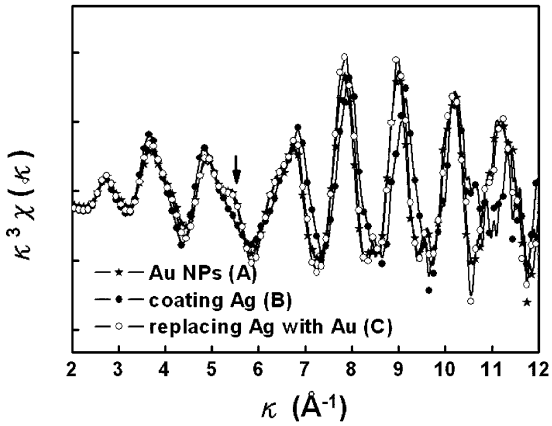

Figure 2. Au L_3 edge EXAFS oscillations for Au nanoparticles (a), Au colloids whose surfaces were coated with shells of pure silver (b), and $Au_{core}Ag_{shell}$ nanoparticles in which Ag was replaced with $HAuCl_4$ (0.4 mL) solution (c). The arrow indicates oscillation caused by the presence of Ag.

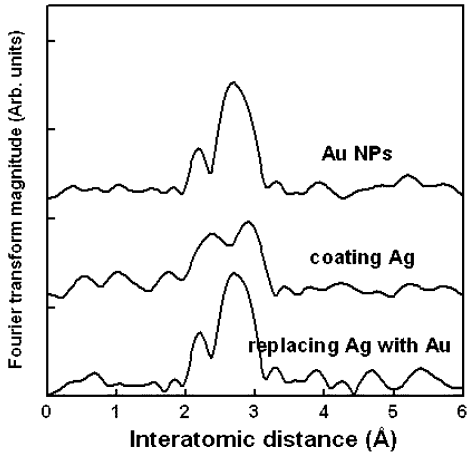

Figure 3. EXAFS analysis of Au nanoparticles, Au colloids whose surfaces have been coated with shells of pure silver, and $Au_{core}Ag_{shell}$ nanoparticles in which Ag was replaced with $HAuCl_4$ (0.4 mL) solution. Fourier transforms of Au L_3 edge $k^3\chi(k)$ EXAFS spectrum of product in each reaction step.

at a lower distance exceeds that at a higher distance as Ag is deposited because interference between Ag and Au oscillations varies. Notably, both peaks come from the first neighbor with a single distance, and they appear to be closer to the actual bond length because of the backscattering phase shift. The doublet component, though, varies with the amount of deposited Ag, suggesting that a significant amount of Ag is present in the nearest-neighbor shell around Au atoms, because of the difference between both the phase shifts and the backscattering functions of Au and Ag. The EXAFS analysis of Au nanoparticles coated with pure silver (b) is characteristic of a two-component structure. When the Ag shell is replaced for the

Downloaded by NATIONAL TAIWAN UNIV on August 10, 2009
Published on September 13, 2006 on http://pubs.acs.org | doi: 10.1021/jp061886h

Downloaded by NATIONAL TAIWAN UNIV on August 10, 2009
Published on September 13, 2006 on http://pubs.acs.org | doi: 10.1021/jp061886h

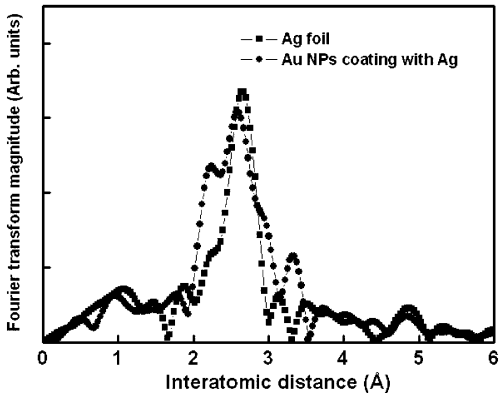

Figure 4. Fourier transforms of the Ag K edge $k^3\chi(k)$ spectrum of Ag foil and Au nanoparticles coated with Ag.

TABLE 1: ExafS Structural Parameters of Au, $Au_{core}Ag_{shell}$, and Nanorattle Nps

sample	path	CN	R (Å)	σ^2 (Å^2)	ΔE (eV)
Au NPs	Au−Au	10.8 (5)	2.86 (2)	0.0089(7)	5.7 (6)
$Au_{core}Ag_{shell}$ NPs (Au L_3)	Au−Au	6.9 (7)	2.83 (6)	0.0088(9)	5.5 (6)
	Au−Ag	3.4 (5)	2.86 (5)	0.0101(9)	−4.8 (8)
$Au_{core}Ag_{shell}$ NPs (Ag K)	Ag−Ag	8.4 (7)	2.87 (5)	0.0103(8)	2.9 (7)
	Ag−Au	3.4 (5)	2.86 (5)	0.0101(9)	−4.0 (4)
nanorattle	Au−Au	11.3 (4)	2.86 (3)	0.0119(8)	4.5 (6)

$HAuCl_4$ solution in $Au_{core}Ag_{shell}$ nanoparticles (c), EXAFS oscillations of the nanorattle are similar to those of Au nanoparticles (Figure 2), because of the absence of a significant amount of Ag in the nearest-neighbor shell around Au. The Fourier transforms of the Au L_3 edge EXAFS spectrum from $Au_{core}Ag_{shell}$ nanoparticles in which Ag is replaced with $HAuCl_4$ solution was consistent with that of pure Au nanoparticles (Figure 3a) or pure gold. This confirms that the shell of the nanorattle was made of pure gold, revealing that these samples had passive shells. X-ray absorption spectroscopy of the Ag K edge was performed to provide further evidence of the absence of Ag atoms in nanorattles. No absorption edge was observed for nanorattles except when the Au nanoparticles were coated with Ag. This result is consistent with the EXAFS analysis of the Au L_3 edge spectra. As shown in Figure 4, the FT-EXAFS spectrum of the Ag K edge of the $Au_{core}Ag_{shell}$ nanoparticles exhibits a distinct interference at the bimetallic interface, unlike that identified by comparison with that of the Ag foil. The FT-EXAFS spectra shown in Figures 3 and 4 were employed to derive the structural parameters based on a two-shell model that involves Au−Au, Au−Ag, Ag−Ag, and Ag−Au shells to characterize the near-range structure near Au and Ag atoms, as presented in Table 1. Notably, the coordination number of Au nanoparticles was slightly smaller than 12 and the Debye−Waller factor significantly exceeded that of gold foil (0.0062), indicating some structural disorder in the nanoparticles. This result demonstrates the nature of the nanomaterials. Detailed curve-fitting analyses of EXAFS results have established the coexistence of Au−Au and Au−Ag bonds in the $Au_{core}Ag_{shell}$ nanoparticles. A simple relationship, $N^{AgAu} = (X_{Au}/X_{Ag})\cdot N^{AuAg}$,[27−29] must be satisfied by the coordination number of the Au atoms around the Ag atoms (N^{AgAu}) and the coordination number of the Ag atoms around the Au atoms (N^{AuAg}). X_{Au} and X_{Ag} represent the atomic fractions of Au and Ag in the colloidal, respectively. Au/Ag bimetallic nanoparticles, as described above, have been fabricated by this method. Notably, the coordination number (Au−Au path) of the $Au_{core}Ag_{shell}$ nanoparticles was significantly smaller than that of the Au nanoparticles, indicating that alloying occurred between Au and Ag atoms at the interface of the Au core and the Ag shell. The coordination numbers of the Au−Ag and Ag−Au paths are sufficiently large to regard some of the alloying as bulk alloying. Alloying can, in principle, be caused by an increase in the diffusion coefficient of the metals, which in turn is related to the decline in the melting point of particles as their size falls in the nanometer region.[32] Size-dependent spontaneous alloying of silver-coated gold nanoparticles has been investigated, and some Au migrated from the core to the shell of the particles.[33] Since the diffusion coefficients of Au nanoparticles are higher than those of the bulk, the density of defects at the bimetallic interface is relatively high. Such defects may promote diffusion by the migration of atoms into vacant defects. Additionally, this alloying may have many causes, including lattice mismatch between the two metals at the interface and excess surface free energy; and others have verified that the shell was made of Au/Ag alloy (Ag-rich). This alloying caused the galvanic replacement reaction between silver and chloroauric acid to reduce the core sizes of the nanorattles because some silver atoms were present in the cores of the rattles, and the surfaces of the cores became rough (Figure 1). A similar result was drawn from the structural refinement of the Ag K edge. As Au-rich core and Ag-rich shell nanoparticles replace Ag shells with $HAuCl_4$ solution, Ag atoms were replaced by Au atoms. The coordination number of the nanorattles slightly increased, suggesting that more Au atoms were present upon the surface of the Au cores. However, the Debye−Waller factor was observably larger than that of the Au nanoparticles. Since the outer shell of the gold was produced in the galvanic replacement reaction between Au^{3+} ions and Ag^0 atoms on the surface, the gold atoms did not have sufficient time to crystallize completely. The morphology, void space, and crystallization of these hollow structures are all determined by the solid templates, which are completely transformed into soluble species by the replacement reaction. As presented by the above EXAFS refinement results, the Ag shell was not single crystalline but Au/Ag alloy. Gold atoms in the part of the shell that was made of Au/Ag alloy became defects as the replacement reaction proceeded, leading to the poor crystallization of the outer shell of gold. Although EXAFS analysis could not directly verify the formation of core−shell and rattle structures, it yielded structural information regarding Au and Ag atoms.

UV−vis Spectral Analysis of Each Product. Since nanostructures of gold and/or silver are well-known to exhibit distinctive SPR features that depend strongly on their shape, composition, and structure, the galvanic replacement reaction between Ag shells and the $HAuCl_4$ solution could also be conveniently followed by the UV−visible spectroscopic method. Figure 5a presents the extinction spectra taken from a set of samples (dispersed in water) that were prepared by adding 0.6 mL of 0.25 M $AgNO_3$ solution to the Au nanoparticles at various time stages. Most interestingly, Figure 5a shows the spectral changes that are associated with the production of $Au_{core}Ag_{shell}$ nanoparticles. The reduction of silver ions and the deposition on the surfaces were accompanied by a shift in a plasmon peak toward the blue region continuously toward 408 nm. The blue shift is attributable to the progressive covering of Au particles by silver layers. Since Ag covered Au, the plasmon band was dominated by Ag. This peak shift may have been caused by a slight increase in void size, and the shifting of the resonance peak toward the blue or red region as the sizes of the gold or silver nanoparticles increase.[34] The alloying of the Au−Ag interface also changes the peak position.[33] The shells of the

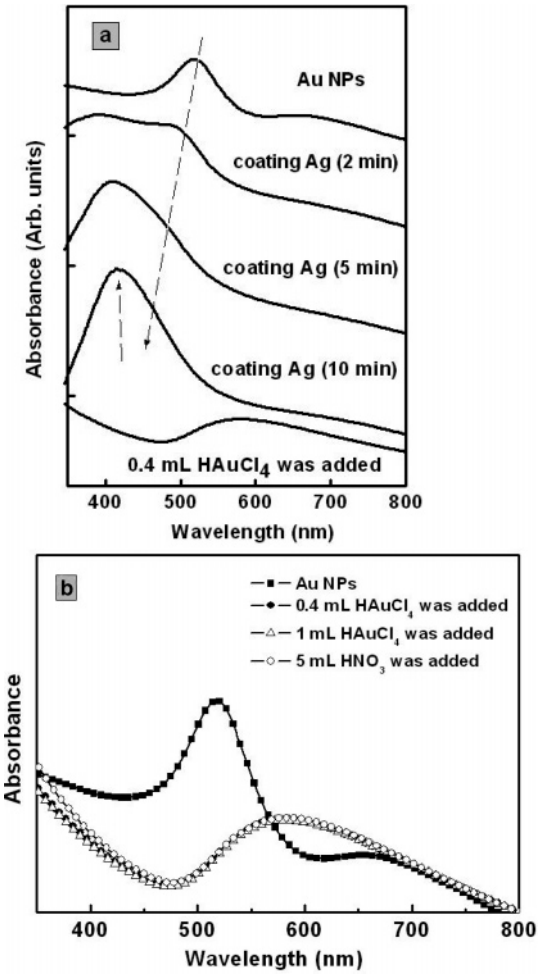

Figure 5. (a) Extinction spectra obtained by adding $AgNO_3$ solution to the Au nanoparticles in various stages; 0.4 mL of $HAuCl_4$ solution was added to Au NPs coated with Ag shell. Time evolves from 0 to 10 min. (b) UV−vis extinction spectra of as-prepared nanorattles after $HAuCl_4$ and HNO_3 solutions were added.

nanoparticles were conveniently prepared by adding various volumes of $AgNO_3$ solution to control the thickness. This result was consistent with the results of TEM and EXAFS. Au_{core}-Ag_{shell} nanostructures could be prepared.

As displayed in Figure 5a, the 408 nm Ag plasmon peak rapidly disappeared and was replaced by a broad peak after 0.4 mL of 0.25 M $HAuCl_4$ solution was added. This result reveals that most of the silver shell of $Au_{core}Ag_{shell}$ colloids had been completely oxidized, even though only a simple electroless plating process was employed. Importantly, this absorption spectrum differed from those reported by Sun.[22,24] Earlier studies demonstrated that the Ag shell was oxidized by $HAuCl_4$ solution to form Au−Ag alloy as $HAuCl_4$ solution was added.[22,24] In these earlier studies, dealloying and fragmentation occurred as more $HAuCl_4$ solution was added.

The formation of silver chloride should be considered here. Silver chloride, that is formed in the replacement reaction, is completely soluble in water under their experimental conditions, because of the solubility product of AgCl at 100 °C.[22,24] In this synthesis, a white solid was observed at the suspension of container at room temperature, suggesting the formation of a AgCl precipitate. The formation of AgCl solid helped remove Ag^+ ions and prevented the gold nanoshells from being contaminated by Ag. A set of experiments were performed to provide further evidence of the effect of temperature in this synthesis. All experimental conditions except temperature were identical across the experiments. Supporting Information Table S1 presents the results of the elemental analysis of nanorattles prepared at room temperature and high temperature. The nanorattles still contained Ag and Cl after they were centrifuged several times to remove the suspended AgCl solid. Accordingly, much of the AgCl solid attached to the surfaces of the nanorattles. When the reaction was conducted under similar conditions, except with the temperature increase from 25 to 95 °C, the larger solubility product of AgCl solid reduced its contamination. The nanorattles were washed with NH_4OH(aq) to remove AgCl solid attached to the surface of the rattles to reduce further contamination of AgCl. As presented in Supporting Information Table S1, the fraction of silver in the final product at high temperature exceeded that of nanorattles at room temperature. Since AgCl solid had a larger solubility product constant, the silver atoms in the reaction system formed Ag^+ rather than solid AgCl. The AgCl solid helped remove the Ag^+ ions and prevented Ag from contaminating the gold nanoshells. Although the low temperature reduced the interdiffusion rate between Ag and Au, potentially yielding a product with a heterogeneous structure, in this study, the silver shell was thin (∼5 nm), and the interdiffusion between Ag and Au occurred easily and then escaped from the nanorattles. Consequently, the shell component of the nanorattles could be controlled by varying the reaction temperature.

More $HAuCl_4$ and HNO_3 solutions were used to demonstrate further the stability of newly synthesized nanorattles. Figure 5b shows the UV−vis extinction spectra of as-prepared nanorattles after $HAuCl_4$ and HNO_3 solutions were added. With further addition of either the 1 mL $HAuCl_4$ solution or the 5 mL HNO_3 solution, the spectra were similar to that obtained when the 0.4 mL $HAuCl_4$ solution was added. These results suggest that the outer shell of the nanorattles was not formed from Au−Ag alloy, that silver was oxidized by excessive $HAuCl_4$ solution, and that the nanorattles had passive shells made of pure gold. These findings agree with the EXAFS analysis of the samples in this investigation.

Conclusions

The galvanic replacement reaction between Ag and $HAuCl_4$ and the electroless deposition of silver were combined to offer a unique route to a number of metal nanostructures. A simple and versatile route for synthesizing nanorattles with pure metal shells was demonstrated. Given the fact that most metals have already been synthesized into nanoparticles, nanowires, nanocubes, and other forms, the same metals can be processed into nanorattle structures using this procedure. The TEM results are consistent with our strategy. $Au_{core}Ag_{shell}$ nanoparticles and nanorattles with a hollow metal shell could be fabricated by this method. EXAFS analysis and UV−vis spectroscopy confirmed the absence of Ag after the Ag shell was replaced with $HAuCl_4$ solution. The shell composition of nanorattles could be easily controlled by varying the reaction temperature. Adding $HAuCl_4$ and HNO_3 solution did not cause the nanostructures to collapse into gold fragments, indicating that the outer shells of the nanorattles were not Au−Ag alloy. Most importantly, the new procedure can be used to prepare nanorattles with pure metal shells (such as Au). Gold nanostructures have received great attention for several decades with widespread applications, and gold surfaces can be readily modified. This new nanostructure of the metal is expected to find use in a range of applications, especially biological.

Acknowledgment. The authors would like to thank the National Science Council of the Republic of China, Taiwan,

Downloaded by NATIONAL TAIWAN UNIV on August 10, 2009
Published on September 13, 2006 on http://pubs.acs.org | doi: 10.1021/jp061886h

for financially supporting this research under Contract No. NSC94-2113-M-002-030.

Supporting Information Available: Elemental analysis of nanorattles following various treatments was conducted using an ICP-AES (Table S1). Best-fitted EXAFS Au L_3 edge spectra of Au nanoparticles, Au nanoparticles coated with Ag shells, nanorattles (Figure S2) and Ag K edge spectra of Au nanoparticles coated with Ag shells (Figure S3). This material is available free of charge via the Internet at http://pubs.acs.org.

References and Notes

(1) (a) Toshima, N.; Yonezawa, T.; Harada, M.; Asakura, K.; Iwasawa, Y. *Chem. Lett.* **1990**, 815. (b) Toshima, N.; Wang, Y. *Langmuir* **1994**, *10*, 4574. (c) Toshima, N.; Wang, Y. *Adv. Mater.* **1994**, *6*, 245. (d) Turkevich, J.; Kim, G. *Science* **1970**, *169*, 873. (e) Schmid, G.; Lehnert, A.; Halm, J. O.; Bovin, J. O. *Angew. Chem., Int. Ed.* **1991**, *30*, 874. (f) Wang, Y.; Toshima, Y. *J. Phys. Chem. B* **1997**, *101*, 5301.

(2) (a) Ahmadi, T. S.; Wang, Z. L.; Green, T. C.; Henglein, A.; El-Sayed, M. A. *Science* **1996**, *272*, 1924. (b) Kamat, P. V. *J. Phys. Chem. B* **2002**, *106*, 7729. (c) Chen, S.; Yang, Y. *J. Am. Chem. Soc.* **2002**, *124*, 5280. (d) Link, S.; Burda, C.; Nikoobakht, B.; El-Sayed, M. A. *Chem. Phys. Lett.* **1999**, *315*, 12. (e) Taton, T. A.; Mirkin, C. A.; Letsinger, R. L. *Science* **2000**, *289*, 1757. (f) Elghanian, R.; Storhoff, J. J.; Mucic, R. C.; Letsinger, R. L.; Mirkin, C. A. *Science* **1997**, *277*, 1078. (g) Mandal, S.; Selvakannan, P. R.; Pasricha, R.; Sastry, M. *J. Am. Chem. Soc.* **2003**, *125*, 8440.

(3) Mulvaney, P. *Langmuir* **1996**, *12*, 788.

(4) Moskovits, M.; Srnova-Sloufova, I.; Vlckova, B. *J. Chem. Phys.* **2002**, *116*, 10435.

(5) Srnova-Sloufova, I.; Lednicky, L.; Gemperle, A.; Gemperlova, J. *Langmuir* **2000**, *16*, 9928.

(6) Kometani, N.; Tsubonishi, M.; Fujita, T.; Asami, K.; Yonezawa, Y. *Langmuir* **2001**, *17*, 578.

(7) Wilson, O. M.; Scott, R. W. J.; Garcia-Martinez, J. C.; Crooks, R. M. *J. Am. Chem. Soc.* **2005**, *127*, 1015.

(8) Henglein, A. *J. Phys. Chem. B* **2000**, *104*, 6683.

(9) Srnova-Sloufova, I.; Vlckova, B.; Bastl, Z.; Hasslett, T. L. *Langmuir* **2004**, *20*, 3407.

(10) Kariuki, N. N.; Luo, J.; Maye, M. M.; Hassan, S. A.; Menard, T.; Naslund, H. R.; Lin, Y.; Wang, C.; Engelhard, M. H.; Zhong, C.-J. *Langmuir* **2004**, *20*, 11240.

(11) Liu, M.; Guyot-Sionnest, P. *J. Phys. Chem. B* **2004**, *108*, 5882.

(12) Mallik, K.; Mandal, M.; Pradhan, N.; Pal, T. *Nano Lett.* **2001**, *1*, 319.

(13) Mallin, M. P.; Murphy, C. J. *Nano Lett.* **2002**, *2*, 1235.

(14) Link, S.; Wang, Z. L.; El-Sayed, M. A. *J. Phys. Chem. B* **1999**, *103*, 3529.

(15) Bergbreiter, D. E. *Angew. Chem., Int. Ed.* **1999**, *38*, 2870.

(16) Jackson, J. B.; Halas, N. J. *J. Phys. Chem. B* **2001**, *105*, 2743.

(17) Pham, T.; Jackson, J. B.; Halas, N. J.; Lee, T. R. *Langmuir* **2002**, *18*, 4915.

(18) Sun, Y.; Mayers, B.; Xia, Y. *Adv. Mater.* **2003**, *15*, 641.

(19) Sun, Y.; Xia, Y. *Adv. Mater.* **2003**, *15*, 695.

(20) Sun, Y.; Xia, Y. *Adv. Mater.* **2004**, *16*, 264.

(21) Sun, Y.; Xia, Y. *Science* **2002**, *298*, 2176.

(22) Sun, Y.; Xia, Y. *Nano Lett.* **2003**, *3*, 1569.

(23) Sun, Y.; Mayers, B. T.; Xia, Y. *Nano Lett.* **2002**, *2*, 481.

(24) Sun, Y.; Wiley, B.; Li, Z.-Y.; Xia, Y. *J. Am. Chem. Soc.* **2004**, *126*, 9399.

(25) Sun, Y.; Xia, Y. *J. Am. Chem. Soc.* **2004**, *126*, 3892.

(26) Kim, S.-W.; Kim, M.; Lee, W. Y.; Hyeon, T. *J. Am. Chem. Soc.* **2002**, *124*, 7642.

(27) Toshima, N.; Harada, M.; Yamazaki, Y.; Asakura, K. *J. Phys. Chem.* **1992**, *96*, 9927.

(28) Harada, M.; Asakura, K.; Toshima, N. *J. Phys. Chem.* **1993**, *97*, 5103.

(29) Toshima, N.; Harada, M.; Yonezawa, T.; Kushihashi, K.; Asakura, K. *J. Phys. Chem.* **1991**, *95*, 7448.

(30) Iwasawa, Y. *X-ray Absorption Fine Structure for Catalysts and Surfaces*; World Scientific: Singapore, 1996.

(31) Jana, N. R.; Gearheart, L.; Murphy, C. J. *Chem. Mater.* **2001**, *13*, 2313.

(32) Buffat, P.; Borel, J.-P. *Phys. Rev. A* **1976**, *13*, 2287.

(33) Shibata, T.; Bunker, B. A.; Zhang, Z.; Meisel, D.; Vardeman, C. F.; Gezelter, J. D. *J. Am. Chem. Soc.* **2002**, *124*, 11989.

(34) (a) Alvarez, M. M.; Khoury, J. T.; Schaaff, T. G.; Shafigullin, M. N.; Vezmar, I.; Whetten, R. L. *J. Phys. Chem. B* **1997**, *101*, 3706. (b) Kreibig, U.; Genzel, L. *Surf. Sci.* **1985**, *156*, 678.

Downloaded by NATIONAL TAIWAN UNIV on August 10, 2009
Published on September 13, 2006 on http://pubs.acs.org | doi: 10.1021/jp061886h